Anisotropic magnetic transport properties and ESR spectra in a tri-layered epitaxial thin-film manganite $La_{2.1}Ca_{1.9}Mn_3O_{10}$

2002 J. Phys.: Condens. Matter 14 211

(http://iopscience.iop.org/0953-8984/14/2/308)

INSTITUTE OF PHYSICS PUBLISHING JOURNAL OF PHYSICS: CONDENSED MATTER

J. Phys.: Condens. Matter **14** (2002) 211–217 PII: S0953-8984(02)29802-1

Anisotropic magnetic transport properties and ESR spectra in a tri-layered epitaxial thin-film manganite $La_{2.1}Ca_{1.9}Mn_3O_{10}$

G Li, H-D Zhou, S-J Feng and X-G Li

Structure Research Laboratory, Department of Materials Science and Engineering, University of Science and Technology of China, Hefei 230026, People's Republic of China

Received 17 October 2001
Published 13 December 2001
Online at stacks.iop.org/JPhysCM/14/211

Abstract

The anisotropic properties of the 30% hole-doped tri-layered manganite film $La_{2.1}Ca_{1.9}Mn_3O_{10}$ have been investigated by means of magnetic transport measurements and electron spin resonance (ESR) experiments carried out in magnetic fields with direction perpendicular and parallel to its surface (the *ab* plane). The results show that the magnetoresistance in a parallel magnetic field is much more prominent than that in a perpendicular one. In addition, the temperature dependence of the resonance field revealed by ESR experiments with respect to the magnetic field directions behaves in different ways. Both the *c*-axis and the *ab* plane anisotropic magnetic interactions and strong demagnetization in the *c*-axis direction should be taken into account to explain these features. The magnetic anisotropy is manifested by the fact that the magnetizations in the parallel and perpendicular magnetic fields deduced from ESR signals are different; the former, which agrees well with a direct dc magnetization measurement in a parallel magnetic field, is much larger than the latter.

1. Introduction

Colossal magnetoresistance (CMR) has been found near the ferromagnetic transition temperature (T_C) in hole-doped manganese oxides with perovskite structure and stimulated investigators to pay considerable attention to understanding their electronic and magnetic properties [1–3]. The ABO_3-type compounds with three-dimensional networks, $Ln_{1-x}A_xMnO_3$ (Ln being rare-earth ions and A divalent cations), such as $La_{1-x}Ca_xMnO_3$ and $La_{1-x}Sr_xMnO_3$, with proper doping level $x \sim 0.3$, have long been known to be conducting ferromagnets. The magnetic interaction is commonly accepted as being the result of a double-exchange mechanism based on the mixed Mn^{3+}/Mn^{4+} valence state. Besides ABO_3-type ($n = \infty$) manganese oxides, the $A_{n+1}B_nO_{3n+1}$-type compound has a layered perovskite structure with two- or quasi-two-dimensional Mn–O–Mn networks. Apart from the $n = 1$ member, which is an antiferromagnet at any doping concentration, the layered manganites with $n = 2$, 3 and

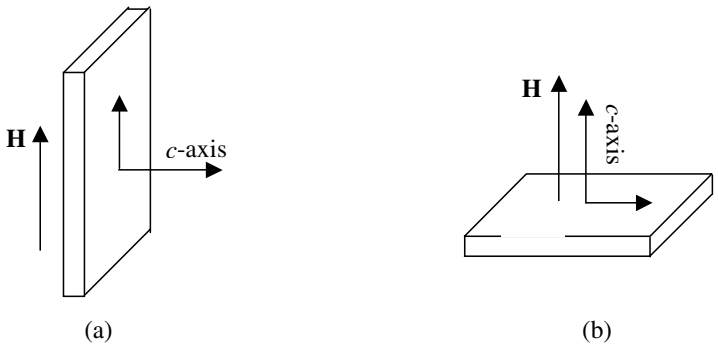

Figure 1. Schematic illustrations for the ESR experiment in magnetic fields with different directions to the sample; (a) $\boldsymbol{H} \perp c$ axis (or $\boldsymbol{H} \parallel ab$ plane), (b) $\boldsymbol{H} \parallel c$ axis (or $\boldsymbol{H} \perp ab$ plane).

$x \sim 0.3$–0.4 are found to be ferromagnets exhibiting CMR effects. Studies [4–8] of the $n = 2$ compounds have shown that they exhibit extraordinary features including MR ratio enhancement, anisotropy in charge transport, magnetization, and the existence of a two-dimensional ferromagnetic ordering at a certain temperature range, etc. It has been recently reported that the $n = 3$ compound [9–11] exhibits similar features to those observed for the $n = 2$ compound. However, the microscopic origin of the features remains unclear, and a unified interpretation to the features with multiple MnO_2 layers in the perovskite family is still under investigation.

Earlier reports [6, 7, 10] demonstrated that the two-dimensional manganites show highly anisotropic magnetic interaction and magnetic transport properties. In this paper, we report the anisotropy in a tri-layered epitaxial thin-film manganite $La_{2.1}Ca_{1.9}Mn_3O_{10}$ by means of magnetic transport measurements and electron spin resonance (ESR) experiments carried out in magnetic fields with directions perpendicular and parallel to its surface (*ab* plane). The results include noticeable anisotropic magnetic transport properties, temperature dependence of resonance fields and linewidth revealed by ESR experiments.

2. Experiment

A single-target magnetron sputtering technique was used for fabricating the thin-film sample of $La_{2.1}Ca_{1.9}Mn_3O_{10}$. The target for the film was a disc with a nominal composition of $La_{2.1}Ca_{1.9}Mn_3O_y$. The thin-film thickness is about 100 nm mounted on the substrate of $LaAlO_3$ (100). X-ray diffraction analysis shows that the film is of single phase with a tetragonal structure and has a *c*-axis orientation with the lattice parameters $a_0 = 0.3865$ nm, $c_0 = 2.675$ nm.

The temperature dependence of the resistivity ρ for the thin film of 5×10 mm^2 was measured by a standard four-probe technique with the current path in the *ab* plane in zero and 0.5 T magnetic fields with directions parallel and perpendicular to its surface. ESR experiments were carried out on a Bruker ER-200D-SRC spectrometer in the X-band at a frequency of 9.47 GHz with temperature ranging from 100 to 250 K. Here, the studied sample is of 1×2 mm^2 size cut from the above-mentioned sample. For each temperature, the magnetic fields vary from 0 to 8000 Gauss with their directions parallel ($\boldsymbol{H} \parallel ab$) and perpendicular ($\boldsymbol{H} \perp ab$) to the *ab* plane of the sample, as shown in figure 1. The dc magnetization as a function of temperature was carried out for the thin-film sample of 5×10 mm^2 on a BHV-55 Vibrating Sample Magnetometer (VSM, Richen Denshi) with the applied magnetic field parallel to the *ab* plane. In order to remove any ambiguity, the resistivity, ESR and magnetization experiments were performed on the same specimen.

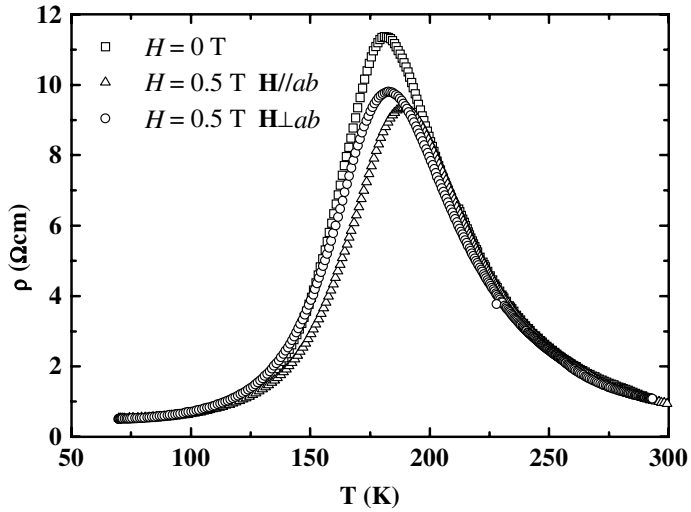

Figure 2. The temperature dependence of resistivity in zero magnetic field and in 0.5 T fields with the direction parallel and perpendicular to the *ab* plane.

3. Results and discussion

Figure 2 shows the temperature dependence of the resistivity ρ in a zero magnetic field. It can be seen that the sample exhibits a metal–insulator (MI) transition with decreasing temperature, the MI transition temperature T_p is about 181 K and the peak resistivity is about 10 Ω cm, which is very similar to the previous study [11]. T_p is close to the ferromagnetic Curie temperature $T_C \sim 184$ K determined by the conventional M^2–T method (as the solid curve shown in figure 5) from a direct dc magnetization measurement. The temperature dependence of magnetoresistance in a low magnetic field of 0.5 T with its direction parallel and perpendicular to the *ab* plane of the sample are also shown in figure 2. Clearly, the fields with different directions to the *ab* plane arouse different changes in resistivity; the parallel field drives the resistivity peak to a higher temperature than the perpendicular field does and brings about a greater magnetoresistance effect. At T_p, the MR ratio (MR $=(\rho(H)-\rho(0))/\rho(H)$) induced by a parallel magnetic field is about 50% larger than that induced by a perpendicular magnetic field although they have the same magnitude.

Such an anisotropy could be firstly understood regarding that the easy-magnetization axis of the sample is in the *ab* plane. The easy magnetization axis in the *ab* plane and anisotropic magnetic transport have been confirmed by dc magnetic magnetization and electronic transport measurements carried on single crystals with layered perovskite structures [4, 9, 12]. The *ab* plane of the sample can be more easily magnetized than that out of the *ab* plane, and the in-plane field can make the magnetic moments of the manganese ions align in the *ab* plane more easily than the perpendicular field does. The alignment of the magnetic moments decreases spin-disorder scattering and suppresses resistivity. However, another reason should be considered, i.e. the static demagnetization along the *c*-axis when the sample is in a ferromagnetic state upon cooling, to explain the different effects aroused by the magnetic fields with different directions to the *ab* plane.

In addition to the resistivity measurements, we had performed ESR studies on the film. Figure 3 show the ESR spectra for the $\boldsymbol{H} \parallel ab$ and $\boldsymbol{H} \perp ab$ cases. One can see that the spectra show different behaviours; for the $\boldsymbol{H} \parallel ab$ case, the resonance field moves gradually to a higher

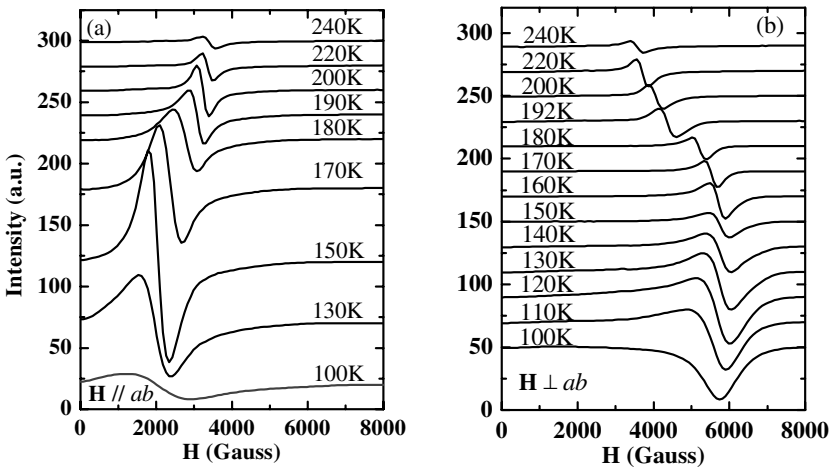

Figure 3. ESR spectra lines at different temperatures in the cases of $\boldsymbol{H} \| ab$ (a) and $\boldsymbol{H} \perp ab$ (b).

field region as temperature increases and changes slightly when temperature arrives at 200 K or above. For the $\boldsymbol{H} \perp ab$ case, in contrast, the resonance field moves gradually to a lower field region upon warming and the resonance field also changes slightly when the temperature reaches 200 K or above. The temperature dependence of resonance fields H_r for the two cases is shown in figure 4(a).

The anisotropic ESR signal for the layered sample film may originate from two main aspects. One aspect is the anisotropic exchange interactions in the *c*-axis (out of *ab* plane) and in the *ab* plane. The Mn–O bond configurations along the *c*-axis and in the *ab* plane are different. According to the previous reports on the anisotropic magnetization of single crystals with layered perovskite structures, the saturated magnetization at ground state in the *ab* plane is much larger than the one along the *c*-axis. This suggests that the ferromagnetic interaction in the *ab* plane is also stronger than that along the *c*-axis. Thus, below T_C, an applied magnetic field in the *ab* plane makes the magnetic moment easily align in the *ab* plane, and the sample shows macro-ferromagnetism and the ferromagnetic resonance appears in the low-field region in ESR signals. This implies that the easy-axis is in the *ab* plane. Due to the insertion of non-magnetic layers of (La Sr)O between the intra-ferromagnetic coupled MnO_2 layers, the inter-ferromagnetic interaction in the *c*-axis direction must be weaker than that in the *ab* plane. Hence, the ESR signal shows anisotropy.

However, one must consider another aspect, the dynamic demagnetization effect, along the *c*-axis for $\boldsymbol{H} \perp ab$ at temperatures around or below T_C. When this occurs, the effective resonance field is now the sum of the external field and the demagnetization field [13, 14]. In this case, the effective resonance field is less than the external applied field. Therefore, to keep resonance at a certain frequency, the measured resonance fields shift to high magnetic fields as temperature decreases below T_C. However, as temperature increases the *ab* plane and *c*-axis ferromagnetic interaction becomes weaker and the *c*-axis demagnetization effect can also be negligible because the ferromagnetism tends to disappear as temperature increases. When the temperature is high enough, the disordered alignment of magnetic moments leads to the appearance of complete paramagnetism and constant resonance fields. The magnetic anisotropy naturally disappears.

It is reasonable to view the film as an infinite plate. In physics [14], below T_C, the sample is in a ferromagnetic state, and when the external magnetic field H is parallel to the *c*-axis, the

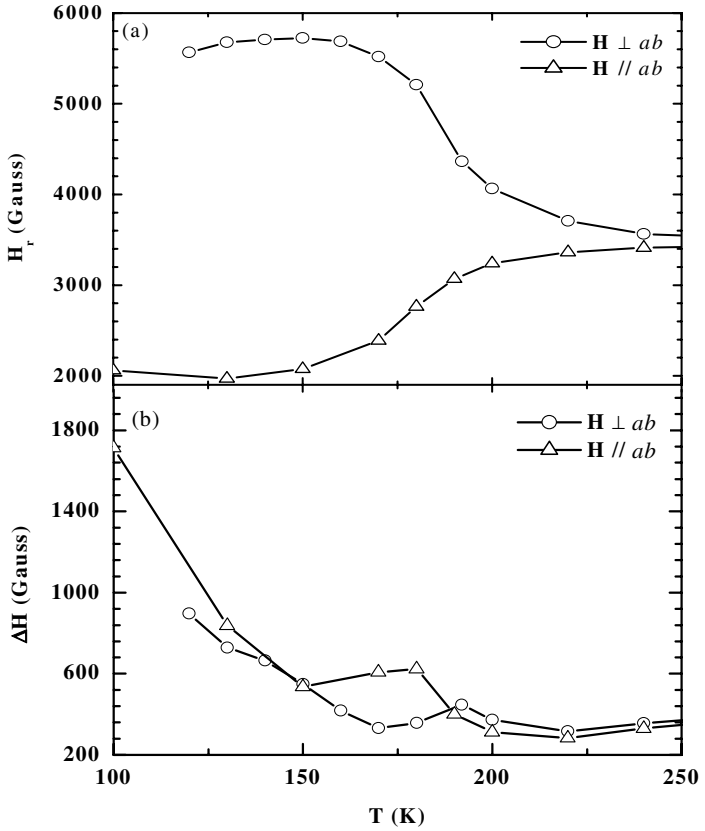

Figure 4. The temperature dependence of resonance field H_r (a) and peak-to-peak linewidth ΔH (b) with respect to field directions.

film shows a strong demagnetization effect along the c-axis and almost a non-demagnetization effect in the ab plane. As shown in figure 1(b), for $\boldsymbol{H} \perp ab$-plane, the effective resonance field H_{eff} is like $H_{\text{eff}} = H - 4\pi M_{\text{EPR}\perp}$, in which H and $M_{\text{ESR}\perp}$ are the applied magnetic field and saturated magnetization perpendicular to the ab plane, respectively. When the applied magnetic field is parallel to the ab plane, although the ab plane demagnetization effect is negligible, the dynamic demagnetization factor along the c axis is still involved to affect the effective resonance field H_{eff} below T_C [14], as $H_{\text{eff}} = [H(H + 4\pi M_{\text{EPR}\parallel})]^{\frac{1}{2}}$, in which $M_{\text{ESR}\parallel}$ is the saturated magnetization parallel to the ab plane. In fact, $M_{\text{ESR}\parallel}$ and $M_{\text{ESR}\perp}$ are dependent on temperature; they are zero when $T > T_C$, and become large as temperature decreases from T_C. According to the resonance condition $h\nu = g\mu_B H_{\text{eff}}$, H_{eff} is invariable with temperature because the frequency is constant. So, one may observe the following evolutions of ESR signals: above T_C, M ($M_{\text{ESR}\parallel}$ and $M_{\text{ESR}\perp}$) is zero; the measured resonance field H_r equals H_{eff} and the sample shows a normal Lorentzian ESR spectrum, and $H_r \approx 3380$ Gauss, no matter whether the external magnetic field is normal to or parallel to the ab plane. Near T_C, M is very small, and demagnetization effect appears, the ESR spectrum now shows a slight distortion for $\boldsymbol{H} \perp ab$. As temperature decreases well below T_C, M becomes larger. To keep resonance, the resonance magnetic fields H_r must shift to a higher region for $\boldsymbol{H} \perp ab$ and to a lower region for $\boldsymbol{H} \parallel ab$. In fact, from this one can derive the value of M.

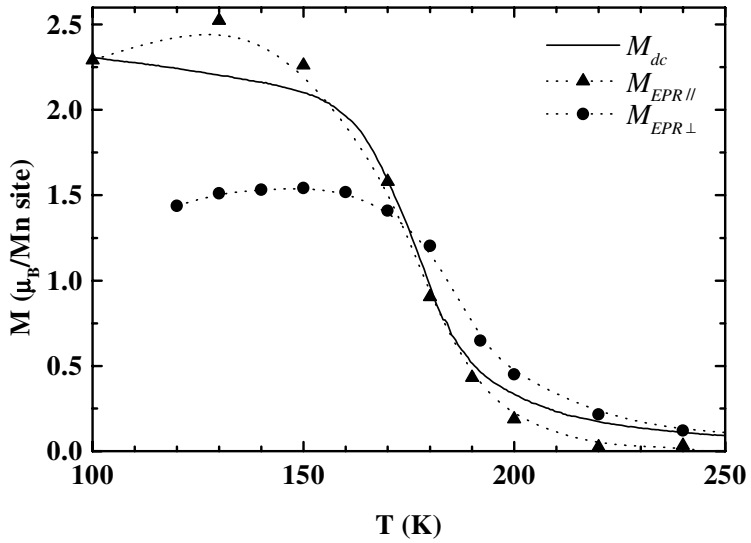

Figure 5. The magnetization curves determined from the VSM measurement and the resonance condition via ESR signals. The solid curve is the dc magnetization (M_{dc}) curve measured via a VSM magnetometer in an applied field of 1000 Gauss with the direction in the *ab* plane. The solid triangle ($M_{\mathrm{ESR}\parallel}$) and circle ($M_{\mathrm{ESR}\perp}$) symbols denote the magnetization as functions of temperature with the magnetic fields direction parallel and perpendicular to the *ab* plane, respectively.

The magnetization in the *ab* plane and out of the *ab* plane, $M_{\mathrm{ESR}\parallel}$ and $M_{\mathrm{ESR}\perp}$, deduced from the resonance condition as a function of temperature, are plotted in figure 5. It is expected that if the magnetization of the film was isotropic, $M_{\mathrm{ESR}\parallel}$ and $M_{\mathrm{ESR}\perp}$ should be identical to each other. It can be seen that, although a transition from paramagnetic to ferromagnetic states occurs at almost the same temperature both for $M_{\mathrm{ESR}\parallel}$ and $M_{\mathrm{ESR}\perp}$, $M_{\mathrm{ESR}\parallel}$ is much larger than $M_{\mathrm{ESR}\perp}$ at $T < T_C$. This is an indication of a large magnetic anisotropy that the hard axis is along the *c*-axis and the *ab* plane is the easy plane, as also seen in bilayered single-crystal manganites $La_{2-2x}Sr_{1+2x}Mn_2O_7$ studied by Moritomo *et al* [4] and Sharma *et al* [15]. We also performed a direct dc magnetization measurement for the film on a VSM magnetometer in an applied field of 1000 Gauss with its direction in the *ab* plane, as shown by the solid curve presented in figure 5. In this case, the static demagnetization effect in the *ab* plane could be neglected. It can be seen that the measured dc magnetization curve agrees well with the $M_{\mathrm{ESR}\parallel}$, in addition the transition temperatures revealed by the three curves are almost the same. This again proves that the anisotropic magnetization and demagnetization are responsible for the observed transport properties and ESR signals.

The temperature dependence of peak-to-peak linewidth ΔH with respect to resonance field directions is shown in figure 4(b). They are slightly different from those found in systems [13, 16] such as $Ln_{1-x}A_xMnO_3$ polycrystalline samples or single crystals with three-dimensional networks, in which the temperature dependence of ΔH shows a stronger linear increase in the paramagnetic region upon warming. The present thin film shows weaker linear temperature dependence in a paramagnetic state ($T > 184$ K) although the linewidth is the same order as that of $Ln_{1-x}A_xMnO_3$. For $Ln_{1-x}A_xMnO_3$ systems, such linear temperature dependence in the high-temperature region is ascribed to the spin–lattice relaxation. The possible explanation for the difference is that the spin–lattice relaxation in the two-dimensional bilayered epitaxial film may be weaker.

In conclusion, we have probed the anisotropy of the 30% hole-doped tri-layered manganite film $La_{2.1}Ca_{1.9}Mn_3O_{10}$ with magnetic transport measurements and ESR experiments carried out in magnetic fields with different directions (perpendicular and parallel) to the thin-film surface. The magnetoresistance measured in a parallel magnetic field is larger than that measured in a perpendicular one. ESR spectra with respect to magnetic field directions behave in a different way. The *c*-axis and *ab* plane transfer interaction and the strong demagnetization in the *c*-axis direction should be considered as the origin of the results.

Acknowledgment

This work was supported by the National Natural Science Foundation of China.

References

[1] Von Helmolt R, Wecker J, Holzapfel B, Schultz L and Samwer K 1993 *Phys. Rev. Lett.* **71** 2331
Jin S, O'bryan H M, Tiefel T H, McCormack M and Rhodes W W 1995 *Appl. Phys. Lett.* **66** 382
Millis A J, Shraiman B I and Mueller R 1996 *Phys. Rev. Lett.* **77** 175
[2] Tokura Y 2000 (ed) *Colossal Magnetoresistive Oxides* (London: Gordon and Breach)
[3] Dagotto E, Hotta T and Moreo A 2001 *Phys. Rep.* **344** 1
[4] Moritomo Y, Tomioka Y, Asamitsu A, Tokura Y and Matsui Y 1996 *Nature* **380** 141
[5] Kimura T, Tomioka Y, Kuwahara H, Asamitsu A, Tamura M and Tokura Y 1996 *Science* **274** 1698
[6] Asano H, Hayakawa J and Matsui M 1996 *Appl. Phys. Lett.* **68** 3638
[7] Asano H, Hayakawa J and Matsui M 1997 *Phys. Rev.* B **56** 5395
[8] Argyriou D N, Mitchell J F, Goodenough J B, Chamaissem O, Short S and Joegensen J D 1997 *Phys. Rev. Lett.* **78** 1568
[9] Okuda T, Kimura T and Tokura Y 1999 *Phys. Rev.* B **60** 3370
[10] Asano H, Hayakawa J and Matsui M 1997 *Appl. Phys. Lett.* **71** 844
[11] Asano H, Hayakawa J and Matsui M 1998 *Phys. Rev.* B **57** 1052
[12] Bader S D, Osgood R M III, Miller D J, Mitchell J F and Jiang J S 1998 *J. Appl. Phys.* **83** 6385
[13] Rubinstein M, Gillespie D J, Snyder J E and Tritt T M 1997 *Phys. Rev.* B **56** 5412
[14] Kittel C 1976 *Introduction to Solid State Physics* 4th edn (New York: Wiley)
[15] Sharma R P, Fournier P, Greene R L, Venkatesan T, Mitchell J F and Miller D 1998 *J. Appl. Phys.* **83** 7351
[16] Oseroff S B, Trikachvili M, Singley I, Ali S, Cheong S W and Schultz S 1996 *Phys. Rev.* B **53** 6521
Rettori C, Rao D, Singley J, Kidwell D, Oseroff S B, Causa M T, Neumeier J J, McClellan K J, Cheong S W and Shultz S 1997 *Phys. Rev.* B **55** 3083
Lofland S E, Kim P, Dahiroc P, Bhagat S M, Tyagi S D, Karabashev S G, Shulyatev D A, Arsenov A A and Mukovskii Y 1997 *Phys. Lett.* A **233** 476